Surface-Plasmon-Induced Visible Light Photocatalytic Activity of TiO 2 Nanospheres Decorated by Au Nanoparticles with Controlled Configuration

ARTICLE *in* THE JOURNAL OF PHYSICAL CHEMISTRY C · DECEMBER 2011

Impact Factor: 4.77 · DOI: 10.1021/jp209520m

3 AUTHORS, INCLUDING:

Dongpyo Kim
Chungnam National University
183 PUBLICATIONS **2,360** CITATIONS
SEE PROFILE

Dong Ha Kim
Ewha Womans University
136 PUBLICATIONS **3,158** CITATIONS
SEE PROFILE

THE JOURNAL OF PHYSICAL CHEMISTRY C

ARTICLE

pubs.acs.org/JPCC

Surface-Plasmon-Induced Visible Light Photocatalytic Activity of TiO_2 Nanospheres Decorated by Au Nanoparticles with Controlled Configuration

Saji Thomas Kochuveedu,[†] Dong-Pyo Kim,[*,‡] and Dong Ha Kim[*,†]

[†]Department of Chemistry and Nano Science, Division of Molecular and Life Sciences, College of Natural Sciences, Ewha Womans University, 52, Ewhayeodae-gil, Seodaemun-gu, Seoul, Korea

[‡]National Creative Research Center of Applied Microfluidic Chemistry, The Cooperation Center for Industry, University and Research Institute (W1), Chungnam National University, 79 Daehangno, Yusung-gu, Daejeon, Korea 305-764

Supporting Information

ABSTRACT: This work is focused on the development of a surface plasmon-induced visible light active photocatalyst system composed of silica−titania core−shell (SiO_2@TiO_2) nanostructures decorated with Au nanoparticles (Au NPs). The influence of size and distribution of Au NPs on photocatalysis, its fabrication methods, and exploration of the mechanism of visible light activity were investigated. A favorable architecture of SiO_2 beads with a thin layer of TiO_2 was decorated with Au NP arrays having different size and areal density. Surface modification of SiO_2@TiO_2 leads to a viable and homogeneous loading of Au NPs on the surface of TiO_2, which renders visible light-induced photocatalytic activity on the whole TiO_2 surface. An optimized system employing Au NP arrays with 15 nm size and 700/μm^2 density showed best catalytic efficiency due to a synergistic effect of the firm contact between Au NPs and TiO_2 and efficiently coupled SPR excitation. A brief mechanism relating the electron transfer from surface-plasmon-stimulated Au NPs to the conduction band of TiO_2 is proposed.

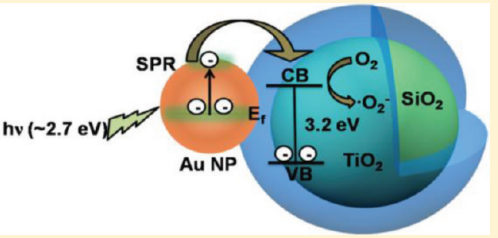

1. INTRODUCTION

Semiconductor-based photocatalysts have attracted growing interest in the field of environmental applications due to their technological importance and superior properties. Owing to its excellent photofunctional properties, chemical stability, and nontoxic nature, TiO_2 is considered to be one of the apt materials for the production of clean energy resources and environmental remediation.[1−6] Nevertheless, the large band gap of 3.2 eV limits its use under UV light, which constitutes only 3% of the total solar spectrum. There have been many efforts, such as dye sensitization,[7−9] incorporation of metal ions,[10−13] and doping with nonmetals,[14−17] to make visible-light-active TiO_2, but the modified materials usually suffer from low efficiency because of low doping concentration. Moreover, it has also been reported that doping may produce recombination center in the lattice. Because the efficiency of photocatalyst is mainly dictated by the lower recombination rate of excitons and effective charge separation, altering the band gap of TiO_2 by doping may not guarantee better catalytic performance, as most of the excitons may recombine before reaching the surface.

Noble metals like Au and Ag have been attracting more attention because they have a wide range of absorption in the visible region based on surface plasmon resonance (SPR), which is due to the collective oscillation of the electrons at the surface of NPs.[18−27] The unique plasmonic absorption features of these noble metal NPs have been used for a variety of applications including chemical sensors,[28−30] biosensors,[31−34] photovoltaics,[35−37] and light emission.[38−40] Whereas a massive amount of work has been carried out to improve photocatalytic activity of TiO_2/noble metal nanostructures under UV light,[3,41,42] exploitation of SPR phenomenon to induce visible light photocatalytic activity of TiO_2 is still a challenging task and lies in a nascent stage. It was evidenced that the electron transfer from Au to TiO_2 is viable under excitation of the plasmon band due to the strong interaction between the environment and oscillating electrons in Au NPs.[43−46] Because the SPR is greatly influenced by the size of the nanoparticles, the efficiency of electron transfer from Au to TiO_2 may be tuned and optimized by altering the size of Au NPs.

Au-loaded TiO_2 photoreaction systems were found to have advantages over other photosensitization methods utilizing organic dyes or metal complexes because the Au deposits are relatively stable under photoillumination in the presence of oxygen.[47] Several representative methods were reported for the introduction of Au NPs on the surface of TiO_2 such as electrolysis,[48] UV photoreduction,[49] and chemical reduction.[50] However, most of the conventional methods failed to offer uniform distribution of Au NPs on the surface of TiO_2, and the incorporated Au NPs are usually loosely attached to the

Received: October 3, 2011
Revised: December 9, 2011
Published: December 27, 2011

Scheme 1. Schematic Illustration of the Preparation Protocol of Core-Shell SiO_2@TiO_2 Nanostructures, Where Silica Bead Is Coated with a Thin Layer of TiO_2 of 15−20 nm Thickness, Followed by Decoration of the SiO_2@TiO_2 Surface with Au NPs of 5, 15, and 30 nm Size[a]

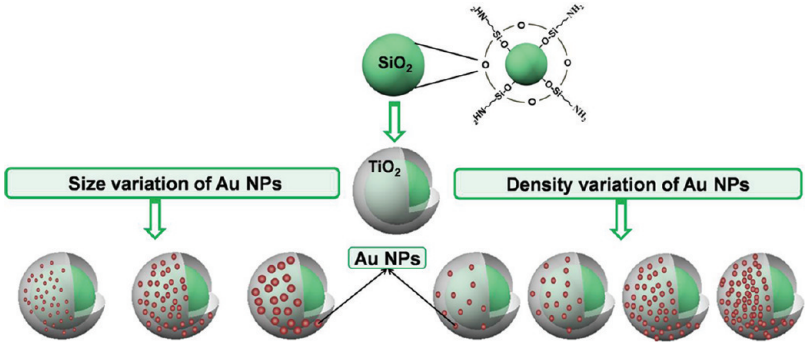

[a] Density of the Au NP arrays on the surface of TiO_2 was adjusted to 24/μm^2, 38/μm^2, 700/μm^2, and 820/μm^2. The green and red spheres represent silica bead and Au NPs, respectively, and the grey coating on silica bead indicates TiO_2 shells.

surface of TiO_2. Wilhelm et al. reported on the photocatalytic efficiency of silica spheres coated with titania prepared by heteroagulation of silica and titania NPs.[51] In this structure, however, the surface of coated titania was uneven, which may cause the decrease in photocatalytic activity. Bian et al. also reported on the enhanced activity and durability of mesoporous core−shell TiO_2 microspheres having encapsulated Au NPs.[52] The size of Au NPs dispersed in TiO_2 matrix reported in this work is uniform enough, but most of the Au NPs exist deep inside of the surface, which contacts the surrounding medium. Therefore, the efficiency of the hybrid TiO_2/Au photocatalyst appears to be relatively low compared with the catalytic efficiency of the broken catalyst samples, and most of works are based on the UV light activity of TiO_2/Au hybrid structure. Recently, Qiao et al. reported on SPR induced visible light activity of nonmetal doped TiO_2/Au nanostructures, but a detailed study on the mechanism of electron transfer between TiO_2 and Au and a systematic study on the effect of the distribution of Au NPs was lacking.[44] Although a limited type of Au-TiO_2 systems has been reported to exhibit visible light activity, a universal paradigm for the design and fabrication of SP-driven visible-light-active semiconductor oxide nanostructures has not been established yet because the architecture and configuration of the previous Au-TiO_2 systems are markedly different from one another.

In this regard, herein we systematically studied on the SP-induced visible light photocatalytic activity using a model system consisting of TiO_2 nanospheres decorated with Au NP arrays having different size range and areal density. This rational design allows us to investigate the evolution of visible light activity in terms of the size and distribution of Au NPs, which have crucial importance in dictating the SPR coupling effect in densely packed metal nanoparticle arrays,[24] and then develop an optimized system for the best photocatalytic efficiency.

2. EXPERIMENTAL SECTION

2.1. Preparation of SiO_2@TiO_2-Au Core@Shell Nanostructure. Monodisperse silica beads were prepared with the procedure previously described by Stöber et al.[53] Tetraethoxysilane (TEOS) was added dropwise to a solution containing ethanol (90 mL), water (4.5 mL), and aqueous ammonia solution (∼ 28%, 15 mL) under stirring at 25 °C for 4 h. The addition procedure of TEOS was repeated four times every 4 h to increase the diameter of silica beads. The reaction was allowed to continue for 6 h at room temperature. 3-Aminopropyltrimethoxysilane (APTMS) (100 μL) was added, and the mixture was refluxed at 85 °C for an additional 4 h. The resultant APTMS-modified silica beads were cleaned by centrifuging and washing with ethanol for three times. The obtained beads were then dried at 60 °C for 12 h. APTMS-modified silica beads (100 mg) were dispersed in ethanol (100 mL) and stirred for 1 h. Titanium tetraisopropoxide (TTIP) (200 μL) was dissolved in ethanol (20 mL). This was then added dropwise to silica bead dispersion, followed by refluxing at 80 °C for 2 h. SiO_2@TiO_2 beads were centrifuged, washed with water, and dried. To decorate the surface of TiO_2 with Au NPs, SiO_2@TiO_2 beads were further modified with APTMS by dispersing SiO_2@TiO_2 beads in ethanol, followed by the addition of APTMS under stirring.

Citrate-stabilized Au NPs of different sizes (5, 15, and 30 nm) were prepared according to the reported methods.[54,55] APTMS-modified TiO_2 beads were then dispersed in citrate-capped Au solution and stirred for different time (1, 2, 4, and 8 h) to control the areal density of Au NPs on the surface of TiO_2. The experiment was repeated with different sizes of Au NPs. SiO_2@TiO_2-Au bead dispersions were washed with water and dried.

2.2. Instruments and Measurements. The morphology of SiO_2@TiO_2-Au beads was investigated using a JEOL JSM-6700F SEM microscope. TEM and EDS measurements were carried out on a JEOL JSM2100-F microscope operated at 100 kV. UV−vis absorbance spectra were measured using a Sinco S-4100 spectrometer. The crystal phase of the powder samples was analyzed using X-ray diffraction with Cu Kα radiation (D/max RA, Rigaku). The accelerating voltage and the applied current were 40 kV and 30 mA, respectively.

2.3. Photocatalytic Activities. We prepared 10 ppm methylene blue (MB) solution was prepared by dissolving 10 mg of MB powder in 1000 mL of distilled water. We mixed 2 mg of catalyst with 30 mL of MB in a quartz container and sonicated for 10 min to get a uniform dispersion. The samples were irradiated under stirring by a Xe lamp (Newport Co., model 66984) equipped with a 420 nm cutoff filter at a power of 450 W as a visible light source. UV−vis absorbance spectroscopy (Varian Cary5000 UV−vis-NIR spectrophotometer) was used to study the change in absorbance maxima of the dye. The same

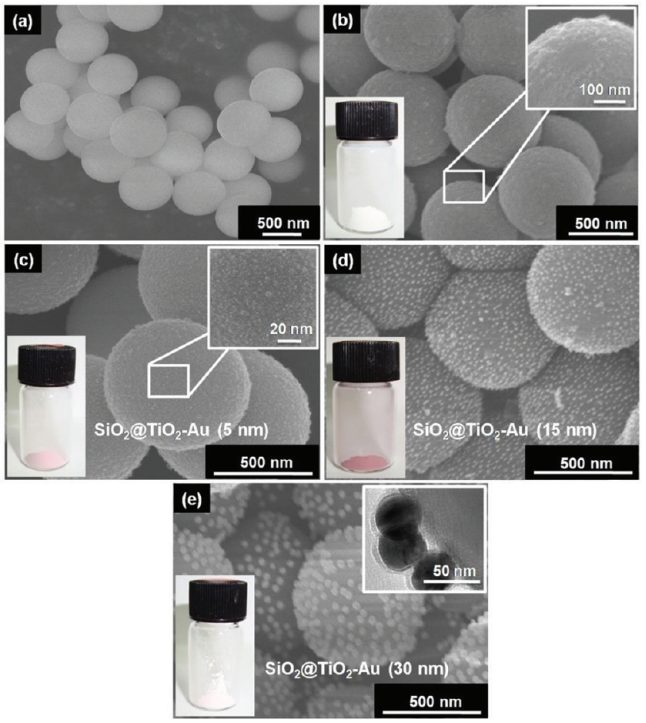

Figure 1. SEM images of (a) silica beads after surface modification with APTMS and (b) silica beads coated with a TiO_2 layer of thickness 15−20 nm (inset is the enlarged image of a selected area). SiO_2@TiO_2 core−shell architecture decorated with Au NPs of different size: 5 nm (c) (magnified image of a selected area in the inset shows a firm contact between the Au NPs and the surface of TiO_2), 15 nm (d), and 30 nm (e). (Inset is the corresponding TEM image.)

procedure was adopted for the degradation study of methyl orange (MO) and *p*-nitrophenol (PNP).

3. RESULTS AND DISCUSSION

The experimental route for the fabrication of SiO_2@TiO_2-Au nanostructures is depicted in Scheme 1. In this study, silica beads of 700 nm size were chosen to ensure easy recovery of the catalyst from the reaction mixture considering a previous report that removal of photocatalysts of smaller size necessitates the use of costly phase separation processes.[56] A uniform thin layer of TiO_2 having thickness of about 15−20 nm was coated onto SiO_2 beads by modifying the surface of SiO_2 using APTMS, followed by sol−gel process. The red spheres on the surface of SiO_2@TiO_2 represent Au NPs on the surface of TiO_2. The firm contact between TiO_2 and Au was assured by surface modification of SiO_2@TiO_2 through APTMS, allowing for more efficient electron transfer. The effect of size and interdistance between the Au NPs on TiO_2-based nanostructures was explored by decorating the TiO_2 surface with Au NPs arrays with controlled architecture.

As shown in Figure 1a, the APTMS-modified SiO_2 beads are of uniform size with a mean diameter of 700 nm. The amine functional groups on the surface of SiO_2 beads aid the formation of uniform thin layer of TiO_2 on SiO_2 without any aggregation (Figure 1b). The photograph of the obtained white powder and the magnified image of a selected area are shown in the insets of Figure 1b. The surface of obtained TiO_2 beads was further modified by APTMS to form sufficient amounts of amine functional groups to which Au NPs can be anchored. Three samples

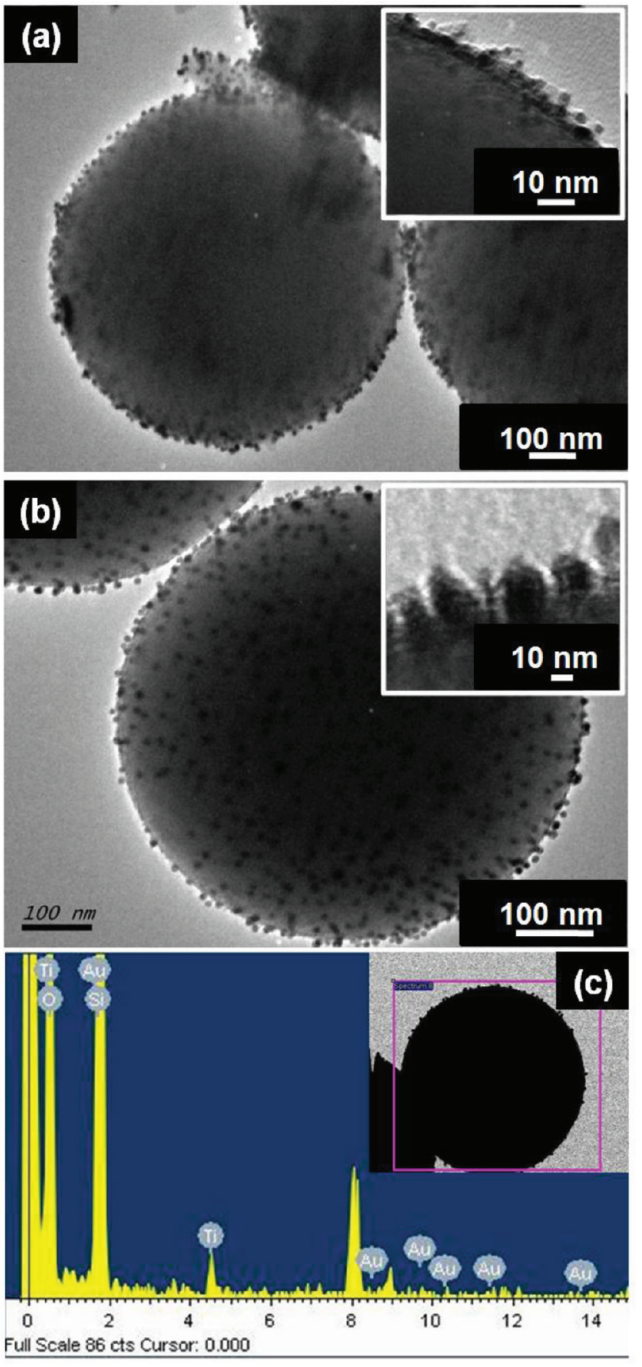

Figure 2. TEM images of SiO_2@TiO_2-Au (5 nm) (a) and SiO_2@TiO_2-Au (15 nm) (b). (Insets are the corresponding magnified images.) (c,d) Selected area and corresponding EDS profile of SiO_2@TiO_2-Au (15 nm), respectively.

decorated with Au NPs of size 5, 15, and 30 nm, that is, SiO_2@TiO_2-Au (5 nm), SiO_2@TiO_2-Au (15 nm), and SiO_2@TiO_2-Au (30 nm), were prepared (Figure 1c−e). The inset of Figure 1c is the enlarged image of a selected area. Because SiO_2@TiO_2-Au-15 showed better and uniform distribution of Au NPs, it was used as a reference system to study the effect of the areal density of Au NPs in the efficiency of catalysis. After decoration with Au NPs, the color of SiO_2@TiO_2 powders was slightly changed to red, indicating that the Au NPs were

attached on the surface of TiO_2 (inset of Figure 1c−e). Au NPs having size of 30 nm are weakly bound to the surface of TiO_2, as confirmed by the TEM image (inset of Figure 1e).

The corresponding TEM image of Figure 1c and TEM and energy-dispersive X-ray spectrum (EDS) of Figure 1d were shown in Figure 2a−c. It is clearly observed that the contact between Au NPs and TiO_2 is rather poor in the case of SiO_2@TiO_2-Au (5 nm) than in the case of SiO_2@TiO_2-Au (15 nm) (inset of Figure 2a,b). It was observed that prolonged outdoor exposure of solution containing 5 nm Au NPs at room temperature led to instability and aggregation of NPs. This may be the reason for the weak contact and nonuniform distribution of 5 nm Au NPs on the surface of TiO_2. In addition to the presence of Au NPs, it is noted that the crystalline phase of TiO_2 is also an important factor to induce better photocatalytic activity because anatase TiO_2 is known to exhibit better reactivity over rutile TiO_2.[57,58] XRD patterns of SiO_2@TiO_2-Au in Figure 3 support the anatase phase of TiO_2, implying that the current system is suitable for the purpose.

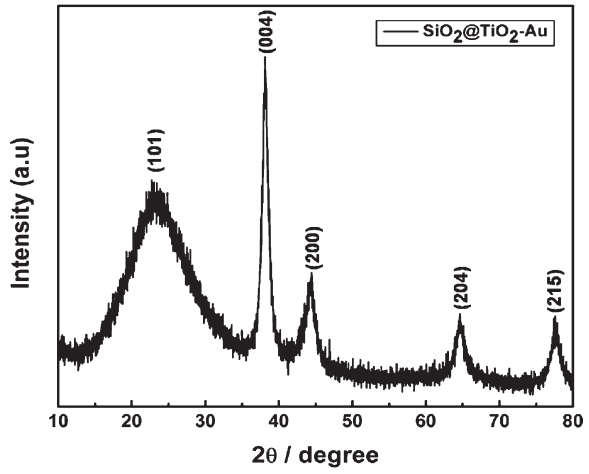

Figure 3. Typical XRD pattern of SiO_2@TiO_2-Au nanostructures.

Next, the effect of the density of Au NPs on TiO_2 surface was investigated using a series of SiO_2@TiO_2-Au (15 nm), where the density was controlled by changing the stirring time of the SiO_2@TiO_2 beads in Au solution. The SEM images show that the density was systematically controlled, as shown in Figure 4a−d. The areal density of the Au NPs on TiO_2 surface was calculated using image processing program ImageJ (Figure S1†and Table S1 in the Supporting Information), and the samples were denoted by SiO_2@TiO_2-Au ($24/\mu m^2$), SiO_2@TiO_2-Au ($38/\mu m^2$), SiO_2@TiO_2-Au ($700/\mu m^2$), and SiO_2@TiO_2-Au ($820/\mu m^2$), respectively. For the SiO_2@TiO_2-Au ($24/\mu m^2$), Au NPs are scarcely scattered on TiO_2 surface (Figure 4a), but better distribution was obtained for the SiO_2@TiO_2-Au ($38/\mu m^2$) (Figure 4b). Homogenous distribution with an almost equal spacing between the individual Au NPs, which is considered to be a critical factor in photocatalysis, was achieved by adjusting the stirring time of the beads in Au solution (Figure 4c). The magnified image of a selected area of SiO_2@TiO_2-Au ($700/\mu m^2$), which clearly shows the uniform distribution of Au NPs without any aggregation, is given in the inset of Figure 4c. The amine functional groups present in the APTMS molecules act as anchoring groups to hold Au NPs to the surface of TiO_2 without any aggregation. Further increase in the immersion time led to an increased portion of aggregates of Au NPs for the SiO_2@TiO_2-Au ($820/\mu m^2$) (Figure 4d).

Figure 5 shows the UV−vis spectra of SiO_2@TiO_2, SiO_2@TiO_2-Au (5 nm), SiO_2@TiO_2-Au (15 nm), and SiO_2@TiO_2-Au (30 nm) nanostructures. The peak at 325 nm is attributed to the characteristic absorption of TiO_2, and the broad peak between 500 and 600 is due to the surface plasmon absorption of Au NPs. It is clearly observed that the SPR absorption band is red-shifted with increasing size of the Au NPs.[54,55,59] The absorption of visible light by Au NPs can produce plasmon-induced photoexcited electrons, and the charge separation can be accomplished by transferring photoexcited electrons to the conduction band of TiO_2.[43−45]

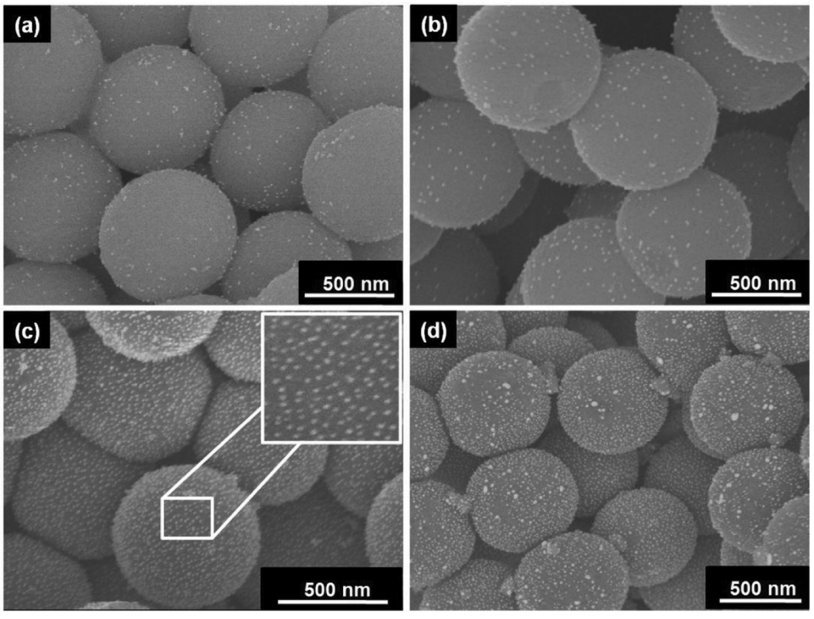

Figure 4. SEM images of SiO_2@TiO_2 decorated with 15 nm Au NPs of different areal density. (a) SiO_2@TiO_2-Au ($24/\mu m^2$), (b) SiO_2@TiO_2-Au ($38/\mu m^2$), (c) SiO_2@TiO_2-Au ($700/\mu m^2$) (inset shows the highest degree of uniform distribution), and (d) SiO_2@TiO_2-Au ($820/\mu m^2$).

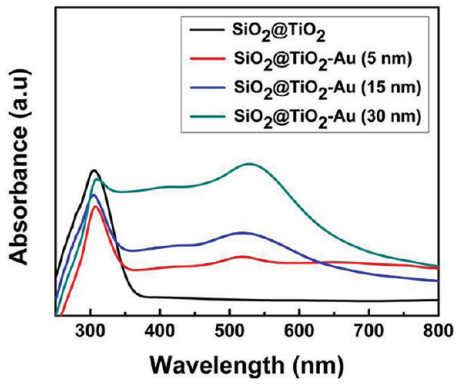

Figure 5. UV−vis absorption spectra of SiO_2@TiO_2 and SiO_2@TiO_2 decorated with Au NPs of different size: SiO_2@TiO_2-Au (5 nm), SiO_2@TiO_2-Au (15 nm), and SiO_2@TiO_2-Au (30 nm).

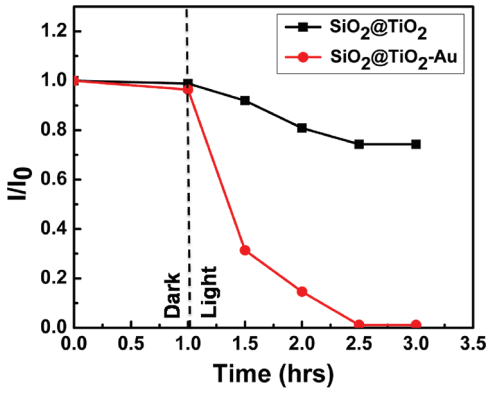

Figure 6. Visible-light-driven photocatalytic degradation of MB on SiO_2@TiO_2 and SiO_2@TiO_2-Au. The photocatalytic efficiency is represented by the absorbance at ~664 nm normalized to that of MB prior to the reaction (I/I_0) versus reaction time.

To explore the visible light activity of our system, we comparatively studied the photocatalytic activities of SiO_2@TiO_2 and SiO_2@TiO_2-Au ($700/\mu m^2$) system using selected targets including MB, MO, and PNP by irradiation with visible light. For typical photocatalysis experiments, 2 mg of the catalyst was dispersed in 30 mL of dye via ultrasonication. The reaction system was then exposed to visible light under stirring. A fixed amount of sample was withdrawn from the stock solution at regular intervals and centrifuged to remove the catalyst, and the specific characteristic absorbance was measured. To facilitate the equilibrium between the adsorption and desorption of dye molecules on the surface of catalyst, we kept the samples in the dark for 1 h before exposure to light. The degradation of MB on SiO_2@TiO_2 was not noticeable, whereas the degradation was complete within 2 h on SiO_2@TiO_2-Au. The ratios of the intensities of the characteristic absorbance peak of MB at a wavelength of about 664 nm were plotted after irradiation with visible light for a specific period of time (I) and prior to irradiation (I_0), as shown in Figure 6. The decrease in absorbance maxima during specific intervals is also provided. (See Figure S2 in the Supporting Information.)

The effect of the size of Au NPs was studied by comparing the photocatalytic activity of SiO_2@TiO_2-Au (5 nm), SiO_2@TiO_2-Au (15 nm), and SiO_2@TiO_2-Au (30 nm), among

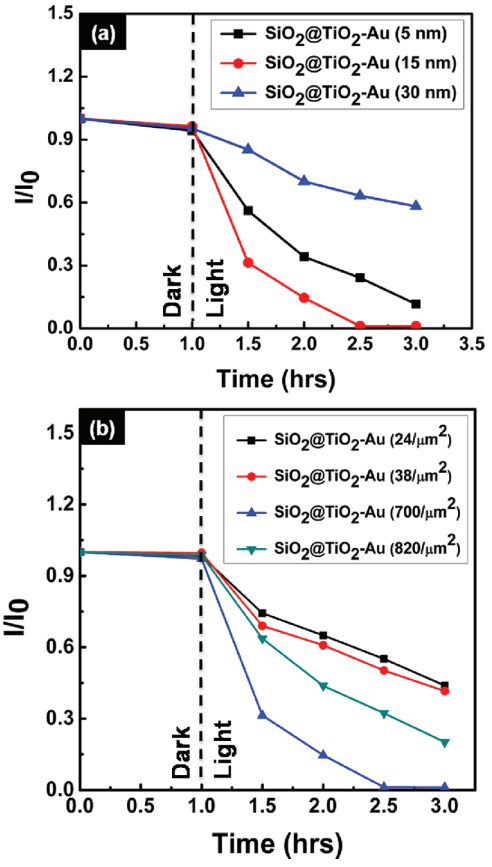

Figure 7. (a) Comparative visible light active photocatalytic degradation study of MB on SiO_2@TiO_2 decorated with Au NPs of different sizes on the surface of TiO_2. Influence of the degree of 15 nm Au NPs loading ($24/\mu m^2$, $38/\mu m^2$, $700/\mu m^2$, and $820/\mu m^2$) on the photocatalytic activity of SiO_2@TiO_2-Au nanostructures studied by using MB as the model system (b).

which SiO_2@TiO_2-Au (15 nm) showed the best catalytic efficiency (Figure 7a). The low photocatalytic efficiency of SiO_2@TiO_2-Au (5 nm) can be due to the poor contact between Au NPs and TiO_2 surface, which was clearly evidenced from the TEM image in Figure 2a. The TEM image of SiO_2@TiO_2-Au (15 nm) shows a close contact between AuNPs and TiO_2, which can lead to the effective transfer of electrons from Au NPs to TiO_2, and this may be the plausible reason for its higher catalytic efficiency. The poor catalytic efficiency of SiO_2@TiO_2-Au (30 nm) is mainly ascribed to a larger size of Au NPs, which restricts the accommodation of more Au NPs on the surface of TiO_2, leading to a smaller amount of energy transfer from Au to TiO_2. The photocatalytic efficiency of noble-metal−semiconductor nanohybrid depends strongly on the size and dispersion of metal NPs and on the extent of contact metal-semiconductor interface.[46] Even though the SPR band of Au and CB of TiO_2 can get closer judging from the shift of SPR peak toward higher wavelength in the case of larger Au NPs, the contact point between Au NPs and TiO_2 can be decreased because of the larger size, as clearly seen in SEM and TEM images. Therefore, it is reasonable to conjecture that the degree of electron transfer from Au NPs to TiO_2 is expected to be relatively less.

To study the influence of the density of Au NPs on photocatalysis, we chose SiO_2@TiO_2-Au (15 nm) as the reference system for further studies. Among the four samples, that is,

dx.doi.org/10.1021/jp209520m |J. Phys. Chem. C 2012, 116, 2500–2506

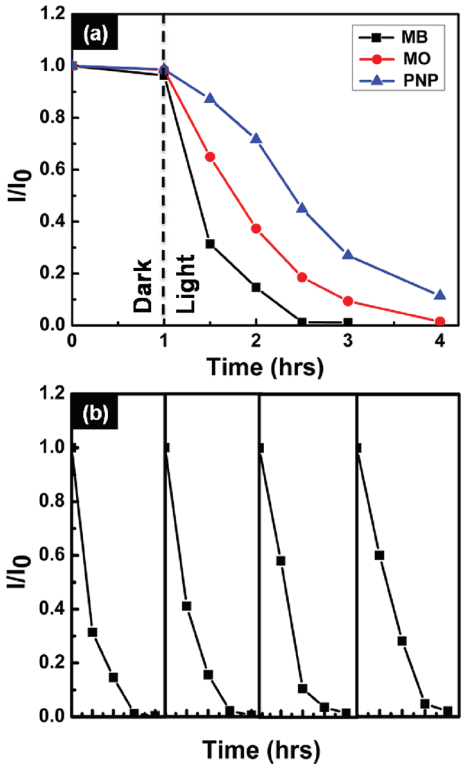

Figure 8. Visible light-induced degradation of different target dyes (a) and recyclability test (b) of photocatalytic degradation of MB on SiO_2@TiO_2-Au (700/μm^2).

SiO_2@TiO_2-Au (24/μm^2), SiO_2@TiO_2-Au (38/μm^2), SiO_2@TiO_2-Au (700/μm^2), and SiO_2@TiO_2-Au (820/μm^2), SiO_2@TiO_2-Au (700/μm^2) showed the best catalytic efficiency (Figure 7b). SEM images of Au-SiO_2@TiO_2-Au (24/μm^2) and SiO_2@TiO_2-Au (38/μm^2) clearly reveal that Au NPs are sparingly decorated on TiO_2 surfaces, so the poor density of Au NPs can promote only a smaller number of electrons to TiO_2. On the contrary, the surface of TiO_2 is decorated with homogenously distributed Au NPs in the case of SiO_2@TiO_2-Au (700/μm^2). The uniform and dense dispersion of Au NPs may lead to a maximized degree of SPR phenomenon, the field of which can then be transferred to the CB of TiO_2, thereby resulting in enhanced catalytic efficiency. When the density of Au NPs is further increased, it may act as a recombination center, which negatively affects the catalytic efficiency.[60] This may explain why SiO_2@TiO_2-Au (820/μm^2), containing the highest density of Au NPs probed in this study, showed comparatively less photocatalytic efficiency.

As a second set of photocatalysis, we compared the photocatalytic activity of different types of target dyes such as MB, MO, and PNP based on the SiO_2@TiO_2-Au (700/μm^2) sample, which was found to exhibit the best catalytic performance. Complete degradation of the MB and MO was obtained within 2 and 3 h, respectively, whereas 90% degradation of PNP was obtained within 3 h (Figure 8a). The decrease in absorption maxima of PNP at 319 nm during regular intervals was plotted. (See Figure S3 in the Supporting Information.) The recyclability of SiO_2@TiO_2-Au (700/μm^2) was also checked by repeating the experiment using the same catalyst with fresh MB (Figure 8b). No obvious reduction in the photocatalytic efficiency was observed even after four cycles, supporting the premise that the system may

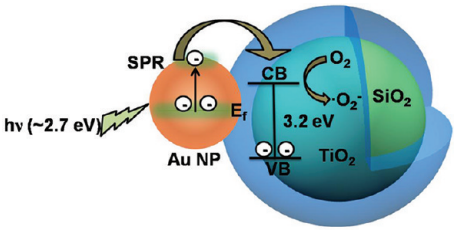

Figure 9. Mechanism of the excitation of surface plasmon of Au NPs, followed by the electron transfer from Au NPs to TiO_2 during the irradiation of visible light.

be adopted as practically viable and stable photocatalysts. The mechanism of the visible light photocatalytic activity of the current SiO_2@TiO_2-Au system is depicted in Figure 9. There are two crucial factors that can assist TiO_2 to work as visible light active catalyst. The first one is the surface plasmon absorption of Au NPs in the visible region, which can be utilized for the visible light irradiation of the catalyst, and the latter is the position of SPR band, which is considered to be above the CB of TiO_2.[44,61,62] Under visible light absorption, the plasmon-induced photoexcited electrons in the Au NPs of SiO_2@TiO_2-Au move through the Au-TiO_2 interface into the CB of TiO_2. The electrons in the CB of TiO_2 can produce superoxide radicals, which can be used for the degradation of organic dyes.

4. CONCLUSIONS

In conclusion, we prepared highly efficient visible-light-active SiO_2@TiO_2-Au photocatalyst through a unsophisticated method. The firm contact of Au NPs on the surface of TiO_2 was ensured by modifying the surface of TiO_2 using APTMS self-assembled monolayers. We have investigated the optimum size and density of Au NPs on the surface of TiO_2 to induce maximum photocatalytic efficiency. Au NP arrays with 15 nm size and 700/μm^2 density showed maximum catalytic efficiency due to a synergistic effect of the firm contact between Au NPs and TiO_2 and the maximized degree of SPR excitation. The visible-light-induced photoexcited Au NPs due to plasmon resonance can inject electrons into the CB of TiO_2 upon excitation. Efficiency of visible light photocatalytic activity of SiO_2@TiO_2-Au was explored using a series of typical volatile organic compounds. The core−shell nanostructures designed and prepared in this study have shown stable and recyclable visible light photocatalytic efficiency, so we believe that our contribution can significantly help to shed a light on the creation of target-customized visible-light-active photocatalytic nanohybrids that may find enormous applications in recent environmental science and technology.

■ ASSOCIATED CONTENT

Supporting Information. Supplementary catalysis profiles. This material is available free of charge via the Internet at http://pubs.acs.org.

■ AUTHOR INFORMATION

Corresponding Author

*Tel: +82-42-821-6695; Fax: +82-42-823-6665; E-mail: dpkim@cnu.ac.kr (D.-P.K.). Tel: +82-2-3277-4124; Fax: +82-2-3277-3419; E-mail: dhkim@ewha.ac.kr (D.H.K.).

■ ACKNOWLEDGMENT

This work was supported by National Research Foundation of Korea grants funded by the Korean Government (20110002494, 2011K000630, 20110001334, and 2010-00134).

■ REFERENCES

(1) Hoffmann, M. R.; Martin, S. T.; Choi, W.; Bahnemannt, D. W. *Chem. Rev.* **1995**, *95*, 69.
(2) Wold, A. *Chem. Mater.* **1993**, *5*, 280.
(3) Devi, L. G.; Kumar, S. G. *J. Phys. Chem. C* **2011**, *115*, 13211.
(4) Kudo, A.; Miseki, Y. *Chem. Soc. Rev.* **2009**, *38*, 253.
(5) Yu, J.; Zhang, L.; Cheng, B.; Su, Y. *J. Phys. Chem. B* **2003**, *107*, 13871.
(6) Kuwahara, Y.; Yamashita, H. *J. Mater. Chem.* **2011**, *21*, 2407.
(7) Chen, X.; Mao, S. S. *Chem. Rev.* **2007**, *107*, 2891.
(8) Kim, W.; Tachikawa, T.; Majima, T.; Choi, W. *J. Phys. Chem. C* **2009**, *113*, 10603.
(9) Füldner, S.; Mild, R.; Siegmund, H. I.; Schroeder, J. A.; Gruber, M.; König, B. *Green Chem.* **2010**, *12*, 400.
(10) Pian, X.-T.; Lin, B.-Z.; Chen, Y.-L.; Kuang, J.-D.; Zhang, K.-Z.; Fu, L.-M. *J. Phys. Chem. C* **2011**, *115*, 6531.
(11) Anpo, M.; Takeuchi, M. *J. Catal.* **2003**, *216*, 505.
(12) Yamashita, H.; Harada, M.; Misaka, J.; Takeuchi, M.; Ikeue, K.; Anpo, M. *J. Photochem. Photobiol., A* **2002**, *148*, 257.
(13) Sakthivel, S.; Kisch, H. *Angew. Chem., Int. Ed.* **2003**, *42*, 4908.
(14) Park, Y.; Kim, W.; Park, H.; Tachikawa, T.; Majima, T.; Choi, W. *Appl. Catal., B* **2009**, *91*, 355.
(15) Chen, X.; Liu, L.; Yu, P. Y.; Mao, S. S. *Science* **2011**, *331*, 746.
(16) Zhang, J.; Wu, Y.; Xing, M.; Leghari, S. A. K.; Sajjad, S. *Energy Environ. Sci.* **2010**, *3*, 715.
(17) Khan, S. U. M.; Al-Shahry, M.; Ingler, W. B., Jr. *Science* **2002**, *297*, 2243.
(18) Murray, W. A.; William, W. L. *Adv. Mater.* **2007**, *19*, 3771.
(19) Hutter, E.; Fendler, J. H. *Adv. Mater.* **2004**, *16*, 1685.
(20) Henry, A. -I.; Bingham, J. M.; Ringe, E.; Marks, L. D.; Schatz, G. C.; Duyne, R. P. V *J. Phys. Chem. C* **2011**, *115*, 9291.
(21) Sardar, R.; Funston, A. F.; Mulvaney, P.; Murray, R. W. *Langmuir* **2009**, *25*, 13840.
(22) Eustis, S.; El-Sayed, M. A. *Chem. Soc. Rev.* **2006**, *35*, 209.
(23) Xia, Y.; Halas, N. J. *MRS Bull.* **2005**, *30*, 338.
(24) Halas, N. J.; Lal, S.; Chang, W. S.; Link, S.; Nodlander, P. *Chem. Rev.* **2011**, *111*, 3913.
(25) William, L. B.; Dereux, A.; Ebbesen, T. W. *Nature* **2003**, *424*, 824.
(26) Murphy, C. J.; Sau, T. K.; Gole, A. M.; Orendorff, C. J.; Gao, J.; Gou, L.; Hunyadi, S. E.; Li, T. *J. Phys. Chem. B* **2005**, *109*, 13857.
(27) Noguez, C. *J. Phys. Chem. C* **2007**, *111*, 3806.
(28) Iga, M.; Seki, A.; Watanabe, K. *Sens. Actuators, B* **2005**, *106*, 363.
(29) Sharma, A. K.; Gupta, B. D. *Nanotechnology* **2006**, *17*, 124.
(30) Cheng, S.-F.; Chau, L.-K. *Anal. Chem.* **2003**, *75*, 16.
(31) Homola, J. *Chem. Rev.* **2008**, *108*, 462.
(32) Law, W. -C.; Yong, K. -T.; Baev, A.; Prasad, P. N. *ACS Nano* **2011**, *5*, 4858.
(33) Prabhakar, N.; Arora, K.; Arya, S. K.; Solanki, P. R.; Iwamoto, M.; Singh, H.; Malhotra, B. D. *Analyst* **2008**, *133*, 1587.
(34) Gradess, R.; Abargues, R.; Habbou, A.; Canet-Ferrer, J.; Pedrueza, E.; Russell, A.; Valdés, J. L.; Martínez-Pastor, J. P. *J. Mater. Chem.* **2009**, *19*, 9233.
(35) Brown, M. D.; Suteewong, T.; Kumar, R. S. S.; D'Innocenzo, V.; Petrozza, A.; Lee, M. M.; Wiesner, U.; Snaith, H. J. *Nano Lett.* **2011**, *11*, 48.
(36) Tian, Y.; Tatsuma, T. *Chem. Commun.* **2004**, 1810.
(37) Hägglund, C.; Zäch, M.; Kasemo, B. *Appl. Phys. Lett.* **2008**, *92*, 013113.
(38) Lai, C. W.; An, J.; Ong, H. C. *Appl. Phys. Lett.* **2005**, *86*, 251105.
(39) Lin, H. Y.; Cheng, C. L.; Chou, Y. Y.; Huang, L. L.; Chen, Y. F. *Opt. Express* **2006**, *14*, 2372.
(40) Dhas, V.; Muduli, S.; Lee, W.; Han, S. H.; Ogale, S. *Appl. Phys. Lett.* **2008**, *93*, 243108.
(41) Subramanian, V.; Wolf, E. E.; Kamat, P. V. *Langmuir* **2003**, *19*, 469.
(42) Cha, M. -A.; Shin, C.; Kannaiyan, D.; Jang, Y. H.; Kochuveedu, S. T.; Ryu, D. Y.; Kim, D. H. *J. Mater. Chem.* **2009**, *19*, 7245.
(43) Furube, A.; Du, L.; Hara, K.; Katoh, R.; Tachiya, M. *J. Am. Chem. Soc.* **2007**, *129*, 14852.
(44) Zhang, Q.; Lima, D. Q.; Lee, I.; Zaera, F.; Chi, M.; Yin, Y. *Angew. Chem.* **2011**, *23*, 7226.
(45) Bian, Z.; Zhu, J.; Cao, F.; Lu, Y.; Li, H. *Chem. Commun.* **2009**, 3789.
(46) Zheng, Z.; Huang, B.; Qin, X.; Zhang, X.; Dai, Y.; Whangbo, M. -H. *J. Mater. Chem.* **2011**, *21*, 9079.
(47) Chatterjee, D.; Dasgupta, S. *J. Photochem. Photobiol., C* **2005**, *6*, 186.
(48) Hosseini, M.; Momeni, M. M.; Faraji, M. *J. Mol. Catal. A: Chem.* **2011**, *335*, 199.
(49) Wang, X.; Caruso, R. A. *J. Mater. Chem.* **2011**, *21*, 20.
(50) Hidalgo, M. C.; Maicu, M.; Navió, J. A.; Colón, G. *J. Phys. Chem. C* **2009**, *113*, 12840.
(51) Wilhelm, P.; Stephan, D. *J. Photochem. Photobiol., A* **2007**, *185*, 19.
(52) Bian, Z; Zhu, J.; Cao, F.; Lu, Y.; Li, H. *Chem. Commun.* **2009**, 3789.
(53) Stöber, W.; Fink, A.; Bohn, E. *J. Colloid Interface Sci.* **1968**, *26*, 62.
(54) Kimling, J.; Maier, M.; Okenve, B.; Kotaidis, V.; Ballot, H.; Plech, P. *J. Phys. Chem. B* **2006**, *110*, 15700.
(55) Ziegler, C.; Eychmüller, A. *J. Phys. Chem. B* **2011**, *115*, 4502.
(56) Fabiyi, M. E.; Skelton, R. L. *J. Photochem. Photobiol., A* **2000**, *132*, 121.
(57) Sclafani, A.; Herrmann, J. M. *J. Phys. Chem.* **1996**, *100*, 13655.
(58) Xu, M.; Gao, Y.; Moreno, E. M.; Kunst, M.; Muhler, M.; Wang, Y.; Idriss, H.; Wöll, C. *Phys. Rev. Lett.* **2011**, *106*, 138302.
(59) Rodríguez, F. J. R.; Pérez, J. J.; de Abajo, F. J. G.; Liz-Marzán, L. M. *Langmuir* **2006**, *22*, 7007.
(60) Wu, Y.; Liu, H.; Zhang, J.; Chen, F. *J. Phys. Chem. C* **2009**, *113*, 14689.
(61) Tian, Y.; Tatsuma, T. *J. Am. Chem. Soc.* **2005**, *127*, 7632.
(62) Yu, K.; Tianw, Y.; Tatsuma, T. *Phys. Chem. Chem. Phys.* **2006**, *8*, 5417.